Journal of Hydrology 528 (2015) 152–160

Contents lists available at ScienceDirect

Journal of Hydrology

journal homepage: www.elsevier.com/locate/jhydrol

Regional temporal persistence of dried soil layer along south–north transect of the Loess Plateau, China

Xiaoxu Jia [a], Ming'an Shao [a,b,*], Chencheng Zhang [b], Chunlei Zhao [b,c]

[a] Key Laboratory of Ecosystem Network Observation and Modeling, Institute of Geographic Sciences and Natural Resources Research, Chinese Academy of Sciences, Beijing 100101, China
[b] State Key Laboratory of Soil Erosion and Dryland Farming on the Loess Plateau, Northwest A&F University, Yangling 712100, China
[c] College of Natural Resources and Environment, Northwest A&F University, Yangling 712100, China

ARTICLE INFO

Article history:
Received 27 March 2015
Received in revised form 12 June 2015
Accepted 14 June 2015
Available online 17 June 2015
This manuscript was handled by Konstantine P. Georgakakos, Editor-in-Chief, with the assistance of Joanna Crowe Curran, Associate Editor

Keywords:
Soil desiccation
Regional transect
Temporal persistence
Spatial distribution
The Loess Plateau

SUMMARY

The occurrence of dried soil layer (DSL) threatens the sustainable development of restored ecosystems in the Loess Plateau of China. Knowledge of the regional spatiotemporal characteristics of DSL in water-deficient regions is critical for optimal water management and vegetation restoration. This study assessed regional temporal persistence of DSL using Spearman's rank correlation coefficient (r_s) and relative difference (RD) analyses and determined the dominant driving factors. Two DSL evaluation indices [DSL thickness (DSLT) and DSL soil water content (DSL-SWC)] were calculated by measuring volumetric SWC of the 0–500 cm soil layer at 86 locations along a south–north regional transect of the Loess Plateau in 2013–2014.

Based on the study, there was DSL formation at most of the sites (61 out of 86 sites) along the transect. The level of DSL was severe, with mean DSLT of 273 cm and mean DSL-SWC of only 10.8% (v/v) [field capacity (FC) = 22.5% (v/v)]. Mean DSL-SWC generally decreased from south to north, while no obvious trend was noted in DSLT along the transect. Derived r_s values indicated a good temporal persistence of spatial patterns of DSL. Also RD analysis showed that DSL with thicker DSLT and/or lower DSL-SWC had much stronger temporal persistence, implying higher possibility for the formation of permanent DSL. The representative locations of each DSL index well represented the regional means of DSLT and DSL-SWC. This suggested that there was the feasibility of directly estimating regional patterns of DSL from theoretical temporal stability. The temporal persistence of DSL patterns was mainly controlled by soil texture, soil organic carbon, field capacity, mean annual precipitation, precipitation seasonal distribution (PSD) and mean annual temperature. We concluded that soil- and climate-related factors dominated regional temporal persistence of DSL. Lower soil water holding capacity, fewer rainfall and more concentrated PSD could intensify the formation and/or development of permanent DSL in the Loess Plateau. This is especially true under worsening global climate change conditions.

1. Introduction

The formation of dried soil layer (DSL) is common phenomenon across the globe. For instance, DSL has been detected in the Loess Plateau of China (Li, 1983), Russia (Yang and Han, 1985), Eastern Amazonia (Jipp et al., 1998) and Southern Australia (Robinson et al., 2006). DSL is recognized as a serious ecological phenomenon in the Loess Plateau (Li, 1983; Chen et al., 2008a; Wang et al., 2010a, 2011a) that has deep loess deposits, unique landscapes and intensive soil and water erosion (Shi and Shao, 2000). The occurrence of DSL potentially interferes with water cycle in soil–plant-atmosphere systems by preventing water flow between shallow (soil moisture) and deep (groundwater) soil layers (Chen et al., 2008a). In addition, prolonged soil desiccation could lead to soil degradation, regional vegetation die-off and aridity of local climatic environments (Breshears et al., 2005; García et al., 2008). Thus DSL affects hydrological conditions and threatens sustainable development of restored ecosystems in the Loess Plateau and beyond. Understanding the development processes of DSL and developing corresponding land management strategies are critical for long-term soil and water ecosystem services in the Loess Plateau and other fragile ecosystems.

* Corresponding author at: Key Laboratory of Ecosystem Network Observation and Modeling, Institute of Geographical Sciences and Natural Resources Research, Chinese Academy of Sciences, Beijing 100101, China. Fax: +86 29 87012210.
E-mail address: shaoma@igsnrr.ac.cn (M. Shao).

http://dx.doi.org/10.1016/j.jhydrol.2015.06.025
0022-1694/

After the first discovery of soil desiccation in the semi-arid regions in Shaanxi and Gansu provinces of China in the 1960s (Li, 1983), numerous studies have since been conducted on DSL in the Loess Plateau. Studies have been conducted on the definition and classification (Yang, 2001; Chen et al., 2008a), formation and development processes (Wang et al., 2009, 2010b), spatial distribution patterns at various scales (Wang et al., 2010a, 2011a, 2012a) and sustainable recovery (Fan et al., 2004; Wang et al., 2011b, 2012b) of DSL.

DSL varies in space and time due to the heterogeneity in soil type, climate, vegetation and topography. Wang et al. (2010a) mapped the spatial distribution of DSL for the entire Loess Plateau, and showed that DSL was generally thicker (>170 cm) in the western and central Loess Plateau region (170–220 cm) than in around the Yellow River and flood plains in the interior irrigation regions. Wang et al. (2010a) concluded that precipitation and soil type were respectively the primary and secondary factors with significant impact on DSL formation and/or development. The rate of formation and thickness of DSL depend largely on vegetation type at regional scale and vegetation age at site scale (Wang et al., 2010b).

Soil desiccation is divided into two types based on dynamic characteristics – temporary type and permanent type (Li, 1983). Permanent DSL typically occurs in arid and semi-arid regions where there is low soil water content due to long-term soil desiccation. Temporary DSL, however, mostly occurs in semi-humid regions. Permanent DSL is difficult to reclaim in the Loess Plateau due to generally limited rainfall, deep groundwater, vegetation consumption and intense evaporation (Wang et al., 2011b). The formation of permanent DSL could have profound and long-term impact on ecological and hydrological processes. Although there exist numerous studies on DSL in the Loess Plateau at various scales, little has been done on the spatiotemporal characteristics of DSL and the related factors at regional scale. The unique regionalized variability of the Loess Plateau makes it specifically difficult to study in terms of sample collection cost and time. Thus there is need for sufficient information on regional temporal persistence of DSL for policy decisions for sustainable soil water management and ecological restoration.

It has recently been demonstrated that the theory of temporal stability is an effective tool for analyzing temporal persistence of properties that vary in space and time. Vachaud et al. (1985) first proposed the concept of temporal stability and defined it as the time-invariant association between spatial location and classical statistical parameters of a given soil property. The definition of the stability of soil water content over time was later expanded to describe temporal persistence of spatial patterns (Kachanoski and de Jong, 1988). This concept has been broadly used to study soil water around the world. This includes the Loess Plateau of China (Hu et al., 2010a,b, 2012; Gao and Shao, 2012; Jia et al., 2013a,b; Liu and Shao, 2014), where soil water content is the most crucial factor for ecological restoration. One of the most useful applications of the concept of temporal persistence is its potential to identify representative locations that rapidly and effectively estimate mean conditions of a given property within the entire study area of interest. Studies on soil water in the Loess Plateau confirm and support the application of temporal persistence. The theory of temporal persistence could therefore provide a useful understanding of regional spatiotemporal characteristics of DSL and the driving factors in the Loess Plateau.

There is widespread occurrence and severity of DSL with potential negative impacts on hydrological processes and ecological environments in the Loess Plateau. There is therefore the need for information on regional spatiotemporal characteristics of DSL and the driving factors. This could guide policy decisions and vegetation restoration strategies to optimize soil and water management. To deepen insight into regional temporal persistence of DSL, this study analyzed neutron probe data collected on 10 occasions along the south–north transect of the Loess Plateau from June 2013 to September 2014. The specific objectives of the study were to deepen insight into the spatiotemporal characteristics of DSL along the south–north transect, and to determine the primary factors that control regional temporal persistence of DSL in the Loess Plateau of China.

2. Materials and methods

2.1. Study area description

This study was conducted in the typical Loess Plateau region. The typical Loess Plateau area covers a total area of *ca.* 430,000 km^2 (Fig. 1), with loess as the most continuous soil in horizontal and vertical space. This area has the most typical loess geomorphic landforms and erosion terrains, such as Yuan (a large flat surface with little or no erosion), ridges, hills and various gullies (Yang et al., 1988). Most of the study area is subject to severe soil and water erosion, causing land degradation and loss of soil fertility. In order to control soil and water erosion and to restore the ecosystem, an extensive ecological rehabilitation program (the "Grain-for-Green") was initiated by the Chinese government in 1999. The program has now been operating for 15 years and the natural environment in most parts of the Plateau is progressively improving.

To effectively measure the characteristics and dynamic properties of DSL at regional scale, a south–north transect (*ca.* 800 km) within latitudes 34.09°N–39.38°N and longitudes 108.62°E–110.32°E was determined in the Loess Plateau (Fig. 1). This transect crosses the moderate-temperate and semi-arid zones, with mean annual precipitation of 400 mm in the north and 620 mm in the south. The mean annual temperature along the transect is 6.8 °C in the north and 12.3 °C in the south.

The soils are mainly of loess with clay-loam as the most common soil texture, sandier soils in the north and clayier soils in the south. The transect has complex topography, including plains, sub-plateaus, hills and gullies with altitude rang of 380–1600 m above mean sea level. From south to north, the land use type generally changes from cropland to forestland and then to grassland. The cropland is often cultivated with winter wheat and summer maize, with irrigation. All the forestlands are artificial with different tree species, including apple (*Maluspumila*), black locust (*Robiniapseudoacacia* L.), apricot (*Armeniacasibirica* L.), jujube (*Zizyphusjujuba*) and korshinsk peashrub (*Caraganakorshinskii*). The grasslands are both artificial, mainly comprised of purple alfalfa (*Medicago sativa* L.), and natural, comprised of *Stipabungeana*, *Lespedeza davurica* and *Heteropappusaltaicus*.

2.2. Sampling location and profile soil water content

Along the south–north transect, 86 aluminum neutron probe access tubes (5.2 m in length) were installed at approximate intervals of 10 km (Fig. 1), measured by vehicle milometer during travel. Each sampling point was randomly selected and located using GPS receiver (5 m precision in the horizontal direction) to represent the main land uses, topography and vegetation types within the range of vision. Volumetric soil water content (SWC) was measured using neutron probe at the 86 locations during the growing season in the period from June 2013 to September 2014. Each measurement process took 3–4 days. There was a total of 10 sampling occasions during the entire sampling period. Slow neutron counts were taken at intervals of 0.2 m to depth of

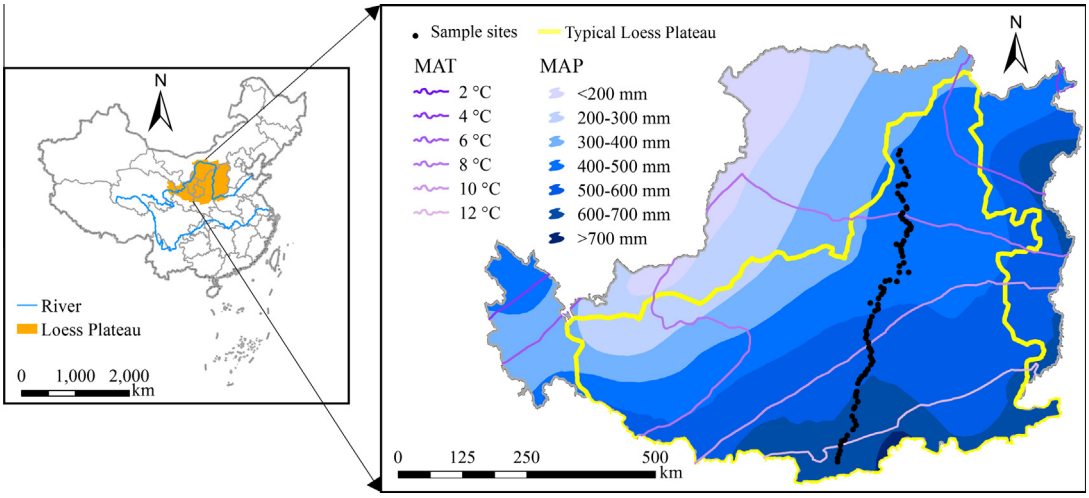

Fig. 1. Map depicting the location of the Loess Plateau in China (left plate) and the south–north transect of the Plateau along with the distributions of mean annual temperature (MAT) and mean annual precipitation (MAP) (right plate). A total of 86 sites were used to determine the south–north transect.

5.0 m. SWC (θ) at each depth was calculated from the slow neutron count rates (CR) using the calibration curve as follows:

$$\theta = 0.5891 \times \mathrm{CR} + 0.0089 \quad (R^2 = 0.93,\ p < 0.001) \tag{1}$$

The calibration curve was obtained for the same area and was considered valid for all soil depth. Based on DSL definition, SWC data in the 0–1.0 m soil layer were not processed. This is because the infiltration depth of loess soil is generally less than 1.0 m in the entire Loess Plateau, especially in dry years (Wang et al., 2010a, 2011a). Thus, consistent with other studies, this study focused on SWC below the 1.0 m soil depth.

2.3. DSL-related factors

2.3.1. Soil

Some 0.5 m away from the access tube at each site, a 40 cm deep pit was excavated to take undisturbed soil samples in the 0–20 cm and 20–40 cm soil layers. The measurements were used to determine saturated soil hydraulic conductivity (Ks, mm/min), field capacity (FC, %) and bulk density (BD, g/cm^3). Ks was determined using the constant-head method (Klute and Dirksen, 1986). SWC at FC (volumetric soil water content at −0.03 MPa) was estimated using the soil water retention curve of Ratliff et al. (1983). Then BD was determined from volume-dry mass relationship for each core sample (Jia et al., 2012).

Disturbed soil samples were also taken for laboratory analyses. The disturbed soil samples were air-dried and divided into two sub-samples. One sub-sample was passed through 1-mm mesh and was analyzed for particle size composition (%) by laser diffraction Mastersizer 2000 (Malvern Instruments, Malvern, England). The other sub-sample was passed through 0.25-mm mesh to determine soil organic carbon (OC, g/kg) using dichromate oxidation method (Nelson and Sommers, 1982). Thus in this study, a total of 5 soil parameters were chosen as factors potentially related to DSL. These factors included Ks, BD, FC, OC and clay content (Clay, <0.002 mm).

2.3.2. Climate

Mean annual precipitation (MAP, mm) and temperature (MAT, °C) for 1953–2013 were derived from the China Meteorological Data Sharing Service System (http://cdc.cma.gov.cn/). This dataset contains climatic data from 73 stations in the Loess Plateau, 64 of which were selected on the basis of the standards set by European Climate Assessment. The station-specific data were interpolated via kriging (at 100 × 100 m^2 resolution) to create a continuous data surface of meteorological factors. Then there was *re*-sampling in *ArcInfo* GIS software (version 9.2) to extract the specific meteorological factor for each sampling site and pixel from the data surface.

Precipitation seasonal distribution (PSD) in the growing season (May to September) is often quantified as the coefficient of variation of the monthly precipitation (CV_{mp}) for each meteorological station (Guo et al., 2012):

$$CV_{mp} = \frac{\sqrt{\frac{1}{5}\sum_{i=5}^{9}(M_i - \overline{M})^2}}{\overline{M}} \tag{2}$$

$$\overline{M} = \frac{1}{5}\sum_{i=5}^{9}(M_i) \tag{3}$$

where M_i is the average precipitation of month i (i is May to September); and $\overline{M}$ is the mean precipitation for the 5 months (May–September). PSD for each sampling site was obtained in the same way as for MAP and MAT.

2.3.3. Topography

The RTK-GPS receiver (5 m location precision) was used to identify the latitude, longitude and elevation (m, above mean sea level) of each site. Slope gradient (°) and aspect (°) was measured using geological compass.

2.3.4. Plants

The investigation of the vegetation at each sampling site was carefully thorough. The investigated variables included tree/grass species, stand density (plants/ha), growth age (years) and vegetation cover (%). In forestlands, three 10 m × 10 m quadrants were established and mean stand density calculated by counting individual trees in each quadrant. Vegetation cover within the quadrants was estimated by visual observation against a 5-m ruler. The growth age of trees was determined by the tree-ring method using Pressler increment borer. In grasslands, three 1 m × 1 m quadrants were established after plant species identification. The plant cover was visually estimated using gridded quadrat frame.

2.4. Dried soil layer indices

Two DSL evaluation indices – dried soil layer thickness (DSLT) and SWC of DSL (DSL-SWC) were treated in this study. DSLT (cm) is calculated as follows (Wang et al., 2010a, 2012a):

$$\mathrm{DSLT} = 20 \times \sum_{i=6}^{n} S(\theta_i - \theta_{\mathrm{SFC}}) \tag{4}$$

where $S(\theta_i - \theta_{\mathrm{SFC}}) = \begin{cases} 0, \theta_i - \theta_{\mathrm{SFC}} > 0 \\ 1, \theta_i - \theta_{\mathrm{SFC}} \leqslant 0 \end{cases}, (i = 6, 7, 8, \ldots, 25), n = 25;$ θ_i is the SWC of the ith soil layer; θ_{SFC} is the SWC at stable field capacity (SFC, generally considered to be equivalent to 60% of FC in the Loess Plateau). After determination of DSLT, DSL-SWC was calculated as the mean of SWC with DSLT.

2.5. Temporal persistence of DSL

Two techniques were used to assess the temporal persistence of DSL – the non-parametric Spearman's rank correlation test (r_s) and relative difference (RD) analysis (Vachaud et al., 1985).

The first technique examined the overall similarity of the spatial patterns DSL for different dates of measurement. Then r_s determined the persistence of the location ranks over time. The r_s value is calculated as follows:

$$r_s = 1 - \frac{6\sum_{i=1}^{N}(R_{ij} - R_{ij'})^2}{N(N^2 - 1)} \tag{5}$$

where N is the number of observation locations; R_{ij} is the rank of DSLT or DSL-SWC observed at location i on day j; and $R_{ij'}$ is the rank of the same variable at the same location for day j'. Values of r_s close to 1 indicate high temporal persistence of DSL.

RD analysis assessed the temporal persistence of DSL for individual observation locations. For each location i, the mean relative difference (MRD), $\overline{\delta}_i$, and the associated standard deviation (SDRD) over time, $\sigma(\delta_i)$, are expressed as:

$$\overline{\delta}_i = \frac{1}{N_j}\sum_{j=1}^{N_j}\frac{\mathrm{DSL}_{ij} - \overline{\mathrm{DSL}_j}}{\overline{\mathrm{DSL}_j}} \tag{6}$$

$$\sigma(\delta_i) = \sqrt{\frac{1}{N_j - 1}\sum_{j=1}^{N_j}\left(\frac{\mathrm{DSL}_{ij} - \overline{\mathrm{DSL}_j}}{\overline{\mathrm{DSL}_j}} - \overline{\delta}_i\right)^2} \tag{7}$$

where DSL_{ij} is the DSLT or DSL-SWC for the ith location at the jth time; $\overline{\mathrm{DSL}_j}$ is the mean DSLT or DSL-SWC of the transect at the jth time. In this method, time-persistent locations tend to have MRD close to zero with minimum associated SDRD over time. In this study, an index of temporal stability (ITS) was used in combination with MRD and the associated SDRD to determine time-persistent sites along the transect (Jacobs et al., 2004; Zhao et al., 2010; Jia et al., 2013a). ITS for each location is computed as follows:

$$\mathrm{ITS}_i = \sqrt{\overline{\delta}_i^2 + \sigma(\delta_i)^2} \tag{8}$$

The site with the strongest temporal persistence has the lowest ITS. In this study, sampling sites with ITS less than 10% were used as time-persistent locations along the transect. To determine the feasibility of directly estimation of mean DSL of the transect from identified time-persistent sites, 4 criteria were used to measure the strength of statistical relatedness of the estimated and measured DSL indices (i.e., DSLT and DSL-SWC). This included the coefficient of determination (R^2), mean error (ME), mean absolute error (MAE)and root mean square error (RMSE), given as:

$$\mathrm{ME} = \frac{1}{N}\sum_{i=1}^{N}(E_i - M_i) \tag{9}$$

$$\mathrm{MAE} = \frac{1}{N}\sum_{i=1}^{N}|(E_i - M_i)| \tag{10}$$

$$\mathrm{RMSE} = \sqrt{\frac{1}{N}\sum_{i=1}^{N}(E_i - M_i)^2} \tag{11}$$

where N is the number of observation point; and E_i and M_i are the estimated and measured values, respectively.

Pearson correlation analysis was used to determine the correlation between MRD, SDRD of DSL indices and environmental factors (i.e., soil, climate, topography and plants). DSL was statistically computed in SPSS 16.0 software.

3. Results and discussion

3.1. Spatial distribution of DSL

In this study, DSL was detected at 61 (71%) of the 86 sampling sites along the south–north transect of the Loess Plateau during the ten observation times from June 2013 to September 2014. The other 25 locations (29%) showed good soil water conditions (SWC > SFC) during the entire experimental period with no DSL formation.

Mean spatial distributions of DSL-SWC and DSLT were determined for the 61 sampling sites with DSL (Fig. 2). The mean DSL-SWC was 10.8% (v/v), significantly lower than the mean FC

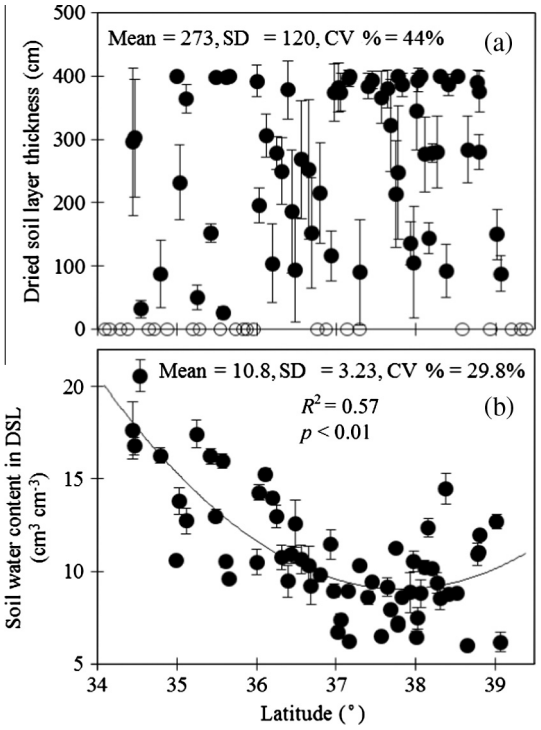

Fig. 2. Spatial distribution and statistical characteristics of dried soil layer thickness (DSLT) (a) and soil water content (SWC) of DSL (DSL-SWC) (b) for the 61 locations (out of 86 sample sites) with detected DSL along the south–north transect of the Loess Plateau. DSLT and DSL-SWC are displayed as mean values for the 10 observations at each site ± standard deviations. Note that mean refers to the spatial mean of DSL for the 61 locations; SD of DSL is the standard deviation of the spatial DSL; CV of DSL is the coefficient of variation of the spatial DSL; empty circles (a) denote sampling locations with 0 cm DSLT, i.e., no dried soil layer.

of 22.5% (v/v). The mean DSLT was 273 cm, showing the severity of DSL at most of the sampling sites.

DSL-SWC generally decreased from 20.6% in the south to 6.0% in the north along the transect. As shown in Fig. 2b, DSL-SWC decreased significantly with increasing latitude. This latitudinal zonality of the spatial pattern of DSL-SWC was mainly related to climate and soil characteristics in the region. Precipitation is the main source of soil moisture in slope lands, plus deep groundwater, MAP and soil water holding capacity were the determinants of SWC at regional scale. The effect of precipitation and soil water holding capacity on DSL-SWC can be explained as the source of input of soil.

Linear regression analysis showed that MAP and FC respectively explained 50% ($p < 0.01$) and 79% ($p < 0.01$) of the spatial variations in DSL-SWC in the study (data not shown). MAP generally decreased from 620 mm in the south to 400 mm in the north (Fig. 1). There was a slight increase in DSL-SWC at the driest end of the transect (Fig. 2b). This highlighted the close relatedness of DSL-SWC and soil properties. Generally, mean Clay and FC of the 0–40 cm soil layer decreased from the south to the north of the transect. There was a slight increase in both properties at the end of the transect from south to north (data not shown). Higher Clay and/or FC meant higher soil water holding capacity. Our results were in agreement with the findings of Wang et al. (2011a), where DSL-SWC was reported to be significantly influenced by soil type and DSL regional distribution pattern related with climatic region and soil texture in the semi-arid Loess Plateau. Jin et al. (2011) also showed that MAP was a decisive factor in determining SWC at regional scale in the Loess Plateau.

Inconsistent with DSL-SWC, no obvious DSLT distribution pattern was detected along the transect (Fig. 2a). This suggested that compared with DSL-SWC, DSLT was driven by more complex processes. Climate, soil, topography and plant factors could invariably influence regional distribution of DSLT. Thus the entire set of DSL data from the 61 sites with DSL was divided into three groups on the basis of land use types – cropland ($n = 3$), forestland ($n = 38$) and grassland ($n = 20$) in order to determine the effects of land use on the spatial patterns of DSLT. The results showed that DSL was generally thicker for forestland (280 cm), and with MAP and mean FC of 513 mm and 22.9% (v/v), respectively. However, DSLT for grassland was 270 cm, and with MAP and mean FC of 450 mm and 19.9% (v/v), respectively. DSLT for cropland was the lowest (210 cm). Thus DSLT under forest (with much higher MAP and soil water holding capacity) was more developed than that under grassland (with lower MAP and soil water holding capacity). This suggested that plants could be critical in determining the distribution patterns of DSLT.

Wang et al. (2011a) showed that the extent of DSL was closely related with the plant species, e.g. tree or grass. This is ascribed to different root distribution patterns of different plants and thus different water uptake capacities, resulting in distinct patterns of development of DSL. Trees generally have deeper root distribution than grass, especially for some exotic tree species with high rate of growth and water uptake. For instance, the maximum depth studied under apple orchard in Changwu County in the south of the Loess Plateau is 12 m (Fan et al., 2004). The depths of soil water depletion by 23-year-old plantedcaragana (*Caraganamicrophylla Lam.*) shrub and 23-year-old planted pine (*Pinustabulaeformis L.*) forest reached were 22.4 and 21.5 m, respectively (Wang et al., 2009). Although no obvious DSLT spatial pattern was detected along the regional transect, a significant relationship was noted between DSLT and DSL-SWC ($R^2 = 0.29$, $p < 0.01$). This was visible in the scatter plot for mean measured DSLT and DSL-SWC (Fig. 3). The plot suggested that the lower DSL-SWC, then the thicker DSLT at regional scale. Irrespectively, the above observations implied that DSL-SWC generally decreased from the south to the north of the transect. This trend was a function of climatic conditions and soil water holding capacity. There was no consistent pattern in DSLT, which could be due to the effect of the plant cover.

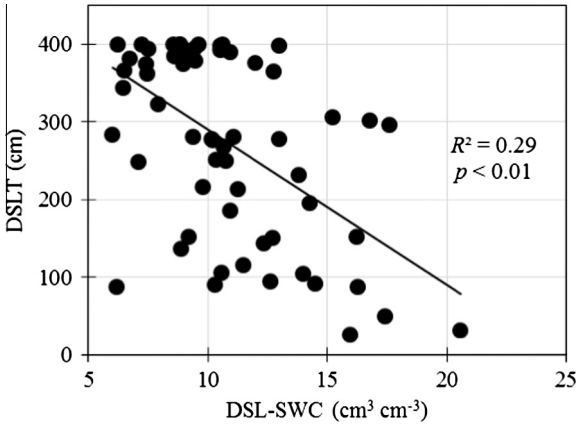

Fig. 3. Plot of correlation between dried soil layer minus soil water content (DSL-SWC) and dried soil layer thickness (DSLT) along the south–north transect of the Loess Plateau ($n = 61$). Note that n is sample size.

3.2. Temporal persistence of DSL

3.2.1. Spearman's rank correlation coefficient

The non-parametric Spearman's rank correlation coefficient (r_s) for the two DSL indices was calculated for the south–north transect. This was used to assess the temporal persistence of the spatial patterns of DSL between the times of measurement in the different months (Table 1). All the coefficients were significant at $p < 0.01$, suggesting strong temporal persistence or similarity of DSLT and DSL-SWC. Also r_s value for DSL-SWC was relatively higher than that for DSLT. For instance, the mean r_s over the whole period of measurement was 0.96 and 0.86 for DSL-SWC and DSLT, respectively. This indicated that temporal persistence of the distribution pattern of DSL-SWC was much stronger than that of DSLT. Higher r_s suggested smaller loss of information between two successive measurement times (Jia et al., 2013b).

3.2.2. Relative difference analysis

Fig. 4 presents the ranked MRD for DSLT and DSL-SWC along with the associated SDRD and the ITS for each sampling site with DSL formation. Generally, the minimum, maximum and range of MRD and the associated SDRD of DSLT were different from those of DSL-SWC. The ranges of MRD and SDRD for DSLT were −90.42% to +46.44% and from 3.73% to 39.72%, respectively (Fig. 4a). The ranges of MRD and SDRD for DSL-SWC were −44.31% to +91.1% and 0.62–12.58%, respectively (Fig. 4b). The range of MRD for DSLT (136.86%) was similar to that of DSL-SWC (135.41%). The almost equal MRD could be ascribed to the similar spatial variability of DSLT and DSL-SWC along the transect (Fig. 2).

The observed ranges of MRD for DSL-SWC were not consistent with those observed in studies at various sampling scales (Vachaud et al., 1985; Martínez-Fernández and Ceballos, 2003; Schneider et al., 2008; Zhao et al., 2010). Schneider et al. (2008) and Brocca et al. (2009) showed that MRD increased at larger sampling scale because of increasing variations in soil, topography and vegetation at larger scales. The range of MRD for DSL-SWC at the regional transect (*ca.* 800 km), however, was relatively smaller than that of MRD (178.9%) for SWC at the 2.0–3.0 m soil depth on small hillslopes (*ca.* 300 m) (Jia et al., 2013a). This observation is inconsistent with the conclusions by Schneider et al. (2008)

Table 1
Spearman rank correlation coefficient (r_s) matrix corresponding to dried soil layer thickness (DSLT) and soil water content (SWC) of DSL (DSL-SWC) at 61 locations (out of 86 sample sites) with DSL for 10 measurement dates along the south–north transect of the Loess Plateau.

	1/6/13	1/8/13	1/9/13	1/10/13	1/11/13	1/4/14	8/6/14	7/7/14	4/8/14	7/9/14
DSLT										
1/6/13	1.00	0.80**	0.77**	0.76**	0.76**	0.71**	0.76**	0.73**	0.76**	0.78**
1/8/13		1.00	0.95**	0.90**	0.88**	0.82**	0.83**	0.80**	0.80**	0.78**
1/9/13			1.00	0.96**	0.94**	0.88**	0.87**	0.83**	0.82**	0.79**
1/10/13				1.00	0.98**	0.93**	0.90**	0.84**	0.84**	0.81**
1/11/13					1.00	0.95**	0.92**	0.86**	0.87**	0.84**
1/4/14						1.00	0.94**	0.89**	0.89**	0.87**
8/6/14							1.00	0.94**	0.94**	0.92**
7/7/14								1.00	0.97**	0.96**
4/8/14									1.00	0.98**
7/9/14										1.00
DSL-SWC										
1/6/13	1.00	0.98**	0.95**	0.96**	0.95**	0.93**	0.92**	0.92**	0.94**	0.94**
1/8/13		1.00	0.98**	0.98**	0.98**	0.96**	0.95**	0.94**	0.95**	0.96***
1/9/13			1.00	0.99**	0.98**	0.96**	0.96**	0.94**	0.94**	0.94**
1/10/13				1.00	0.99**	0.98**	0.97**	0.95**	0.95**	0.95**
1/11/13					1.00	0.99**	0.98**	0.96**	0.96**	0.96**
1/4/14						1.00	0.99**	0.97**	0.97**	0.96**
8/6/14							1.00	0.98**	0.97**	0.97**
7/7/14								1.00	0.99**	0.98**
4/8/14									1.00	0.99**
7/9/14										1.00

** Correlation is significant at the 0.01 level (2-tailed test).

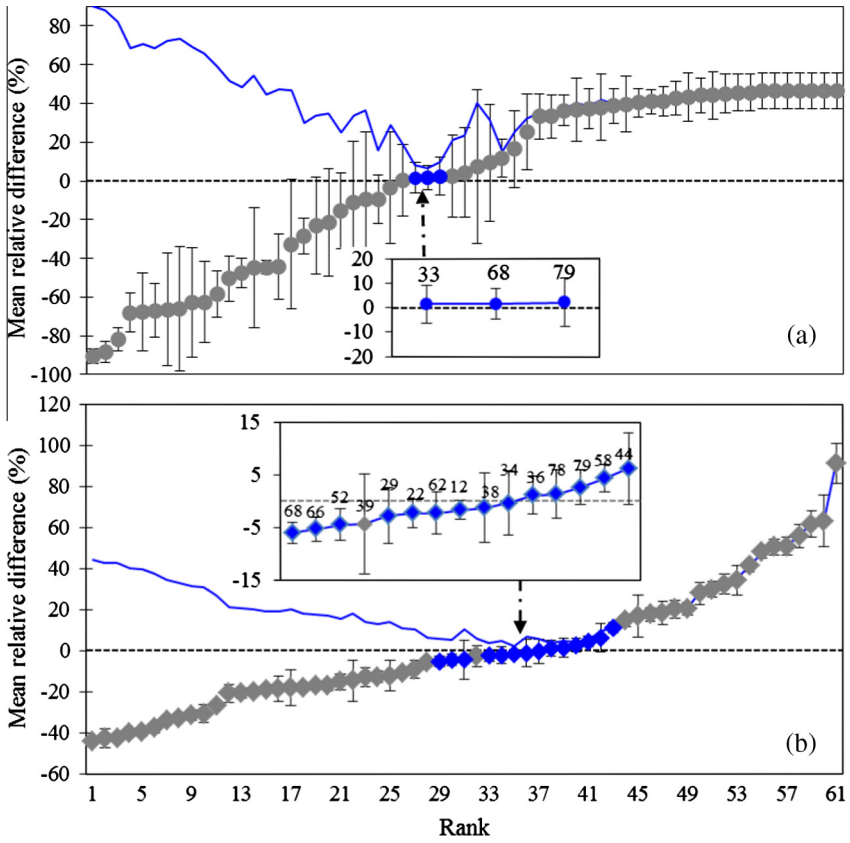

Fig. 4. Ranked mean relative differences in dried soil layer thickness (DSLT) (a) and in dried soil layer minus soil water content (DSL-SWC) (b). Vertical bars represent ± one standard deviation of relative differences; bold curve is the index of temporal stability (ITS); and locations with ITS less than 10% are marked in blue. (For interpretation of the references to color in this figure legend, the reader is referred to the web version of this article.)

and Brocca et al. (2009). This was partly due to differences in the layout of the experiments and also differences in soil, topography and vegetation (Vanderlinden et al., 2011). Also RD analysis of SWC in this study (i.e., SWC of DSL) was different from that in other studies (i.e., SWC of the entire profiles), which could confound MRD range at different scales.

The mean values of SDRD for DSLT and DSL-SWC were different, with only 4.22% for DSL-SWC and 15.38% for DSLT. This suggested that DSL-SWC exhibited a much stronger temporal persistence than DSLT. Assuming that locations with SDRD less than 5% were temporally stable (Starks et al., 2006; Hu et al., 2010b), then the number of time-stable locations of DSL-SWC was relatively higher

than that of DSLT. For instance, the number of locations with SDRD less than 5% for DSL-SWC was 43 (out of the 61 sites). For the DSLT, however, only 2 of the 61 sites were temporally stable (Fig. 4). It was therefore concluded that DSLT was apparently less temporally stable than DSL-SWC. This was because of increased dependence on soil, climatic and vegetation factors at regional scale.

In addition, a significant positive correlation ($p < 0.01$) was detected between mean DSL-SWC and the associated SDRD (Fig. 5a). This suggested that temporal persistence of DSL in relatively drier locations were always more stable than in wetter locations. Conversely, a significant negative correlation ($p = 0.048$) was noted between mean DSLT and the associated SDRD (Fig. 5b). This also suggested that the thicker DSL was, the more persistent was DSL. This observation was consistent with that of Martínez-Fernández and Ceballos (2003) where the temporal stability of SWC was observed to be stronger in dry than in wet conditions. However, Hupet and Vanclooster (2002) and Zhao et al. (2010) observed the opposite relationship.

Irrespectively, sites with lower DSL-SWC and/or thicker DSLT tended to be more temporally stable. This was attributed to weak capillarity of water from shallow to deep soil layer which in turn enhanced temporal persistence of DSL. Stronger temporal persistence implied higher possibility for the formation of permanent DSL. Permanent DSL was stable, with extremely difficult soil water replenishment because of limited rainfall and high vegetation water consumption (Wang et al., 2010b, 2011a). As groundwater was unusable for recovery of soil desiccation due to thick loess deposits, undoing soil desiccation in the Loess Plateau could only be achieved over long period of time (Wang et al., 2011b). Permanent soil desiccation therefore has long-term implications for hydrological processes, sustainable ecological restoration and social stability in the Loess Plateau.

3.2.3. DSL estimation from representative sites

Time-stable locations as sites with ITS less than 10% were used to represent the mean DSLT and DSL-SWC at regional scale. In this study, 3 and 14 locations were identified to represent DSLT and DSL-SWC, respectively (Fig. 4 and Table 2). Thus more time-stable locations were chosen to represent regional transect mean of DSL-SWC than DSLT. We further selected the time-stable sites that were simultaneously representative of DSLT and DSL-SWC. Two sites (68 and 79) were simultaneously representative of estimated mean DSLT and DSL-SWC. Finding a single site that was representative of both mean DSLT and DSL-SWC at the regional transect can reduce labor and cost. However, the accuracy of estimation could not be the best for all representative sites.

Thus we determined the feasibility of estimating DSL using representative sites against four criteria – R^2, ME, MAE and RMSE (Table 2). Site 68 was used to estimate mean DSLT of the transect because it had the lowest ME (5.21), MAE (14.98) and RMSE (17.38). Representative sites with the best accuracy of estimation of DSL-SWC were sites 12 and 36. Also site 68 was representative of mean DSL-SWC, with ME, MAE and RMSE of −0.70, 0.70 and 0.73, respectively (Table 2). Thus in this study, a single time-stable site (68) was said to be representative of both DSLT and DSL-SWC. This was advantageous because it reduced sample size to one and maintained high accuracy of estimation. The study showed the feasibility of directly estimating mean DSLT and DSL-SWC from one representative site at regional scale, closely consistent with other studies (Jacobs et al., 2004; Hu et al., 2010b, 2012; Brocca et al., 2012; Gao and Shao, 2012; Jia et al., 2013a). Schneider et al. (2008) and Liu and Shao (2014) further showed that representative sites were appropriate for estimating mean SWC in multiple year analysis. Nevertheless, there was need for further research on the feasibility of long-term estimation of DSL from a single representative site.

Table 2
Summary statistics of representative of the transect and evaluated estimation accuracy based on4 criteria.[a]

DSL indices	Locations	ITS (%)	R^2	ME	MAE	RMSE
DSLT/cm	33	8.06	0.34	5.21	16.62	20.75
	68	6.42	0.24	5.21	14.98	17.38
	79	9.99	0.14	7.21	22.62	26.97
DSL-SWC/cm^3 cm^{-3}	12	2.39	0.32	−0.23	0.26	0.29
	22	3.57	0.16	−0.30	0.37	0.41
	29	5.90	0.52	−0.34	0.53	0.63
	34	6.04	0.06	−0.09	0.55	0.62
	36	3.80	0.36	0.07	0.31	0.38
	38	6.77	0.15	−0.19	0.63	0.71
	44	9.27	0.15	0.62	0.85	0.94
	52	5.39	0.07	−0.54	0.54	0.62
	58	5.05	0.02	0.41	0.41	0.48
	62	4.62	0.41	−0.30	0.43	0.50
	66	5.83	0.49	−0.63	0.63	0.67
	68	6.33	0.15	−0.70	0.70	0.73
	78	4.82	0.35	0.09	0.40	0.48
	79	4.22	0.03	0.22	0.30	0.40

[a] R^2 is coefficient of determination; ME is mean error; MAE is mean absolute error; RMSE is root mean square error; and ITS is index of temporal stability.

3.3. Factors driving temporal persistence of DSL

Spatial patterns of DSL are related to soil properties (Pollen, 2007), climatic factors (Wang et al., 2012a), topographic factors (Wang et al., 2010a, 2011a) and plant characteristics (Bosch et al., 2006; Wang et al., 2011a). In order to determine the

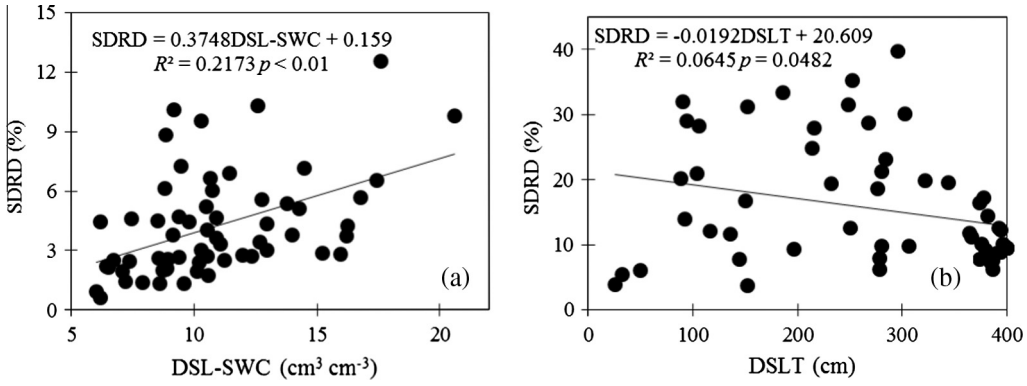

Fig. 5. Plot of linear correlation between standard deviation of relative difference (SDRD) and dried soil layer (DSL) indices for (a) DSL-SWC, and (b) DSLT ($n = 61$). Note that SWC is soil water content; DSLT is dried soil layer thickness; and n is sample size.

Table 3
Pearson correlation analysis for mean relative difference (MRD), standard deviation of relative difference (SDRD) and selected soil, climate, topography and plant factors along the south–north transect of the Loess Plateau.

Environmental variables	MRD		SDRD	
	DSL-SWC	DSLT	DSL-SWC	DSLT
Soil				
Clay content (%)	0.802**	−0.248*	0.376**	−0.072
Soil organic carbon (g kg^{-1})	0.707**	−0.16	0.380**	0.032
Field capacity (%)	0.891**	−0.285*	0.450**	−0.094
Bulk density (g cm^{-3})	−0.094	−0.007	−0.084	−0.217
Saturated hydraulic conductivity (cm min^{-1})	0.055	−0.132	0.137	0.154
Climate				
Mean annual precipitation (mm)	0.708**	−0.385**	0.319*	0.017
Precipitation seasonal distribution (%)	−0.665**	0.167	−0.389**	−0.14
Mean annual temperature (°C)	0.618**	−0.145	0.325*	0.118
Topography				
Elevation (m)	−0.343**	0.024	−0.219	−0.147
Slope aspect (°)	−0.04	−0.027	−0.209	−0.244
Slope gradient (°)	−0.254*	0.099	0.088	0.02
Plants				
Stand density (plants ha^{-1})	−0.174	0.041	−0.05	0.238
Vegetation coverage (%)	0.156	−0.013	0.032	−0.152
Growth age (years)	−0.012	0.101	−0.134	0.211

* Correlation is significant at the 0.05 level (2-tailed).
** Correlation is significant at the 0.01 level (2-tailed); DSL is dried soil layer; DSLT is dried soil layer thickness; and SWC is soil water content.

dependence of temporal persistence of DSL on these variables, a simple correlation analysis was conducted on MRD and SDRD for each DSL index and the selected factors of soil, climate, topography and vegetation (Table 3).

MRD of DSL-SWC was positively correlated with Clay, OC, FC, MAP and MAT. However, it was negatively correlated with PSD, elevation (E) and slope gradient (SG). Except for topographic factors, the correlation between SDRD (of DSL-SWC) and soil/climate-related factors was similar to that between MRD and the factors (Table 3). In contrast to DSL-SWC, MRD (of DSLT) was negatively correlated with Clay, FC and MAP. However, no significant correlation was observed between SDRD (of DSLT) and the various factors. In addition, no significant correlation existed between MRD, SDRD and vegetation properties at regional scale (Table 3). The above observations suggested that soil/climate-related factors could determine regional temporal persistence of DSL-SWC and DSLT in the Loess Plateau. This observation was concurrent with the findings of Hu et al. (2010a), where soil texture significantly affected the temporal stability of SWC. Furthermore, soil OC can significantly improve soil structure, soil water holding capacity and soil infiltration, thereby influencing the spatiotemporal patterns of SWC (Zhao et al., 2010; Biswas and Si, 2011; Jia et al., 2013a). Precipitation (the main source of soil moisture in slope lands in the Loess Plateau) could directly affect soil water replenishment in dried soil layers. This could in turn affect the temporal persistence of the spatial patterns of DSL (Wang et al., 2011a). Furthermore, annual precipitation in the Loess Plateau has been decreasing and air temperature increasing (Wang et al., 2011a, 2012c). This not only decreased precipitation input, but also increased evaporation and potentially increased the severity of DSL in the Loess Plateau.

In addition to MAP, there was significant negative correlation between PSD, MRD and SDRD (for DSL-SWC). This was ascribed to the diverse and complex terrains in the Loess Plateau. The typical landforms in the region are loess "Yuan, Liang and Mao" and various valleys with different magnitudes of erosion. Hills, deep gullies and undulating loess slopes are common landforms of the Loess Plateau landscape (Tsunekawa et al., 2014). Consequently, sparse and more extreme rainfall events without concurrent changes in total precipitation could intensify soil and water erosion, increase runoff water loss, decrease water infiltrate into deep soil layers and thereby enhance temporal persistence of DSL-SWC (Yu, 1992; Yang, 2001; Tsunekawa et al., 2014). The complex terrain could also affect hydrological processes such as overland flow, rainwater infiltration and redistribution, soil water movement in both surface and subsurface layers (Chen et al., 2008b). This could explain the significant correlation between E, SG and MRD (for DSL-SWC). We therefore concluded that low soil water holding capacity, fewer precipitation and more concentrated PSD could intensify the formation of permanent DSL in the Loess Plateau under global climate change.

4. Conclusions

Spatial patterns of DSLT and DSL-SWC along the south–north transect of the Loess Plateau differed significantly at regional scale. Mean DSL-SWC generally decreased from south to north along the transect while no obvious trend existed in DSLT. Spearman's rank correlation coefficient (r_s) and relative difference (RD) analyses showed good temporal persistence of the spatial patterns of both DSLT and DSL-SWC. DSL with thicker DSLT and/or lower DSL-SWC was apparently exhibited much stronger temporal persistence. From ITS values, one time-persistent site simultaneously represented regional transect of mean DSLT and DSL-SWC, which was further verified by four other criteria – R^2, ME, MAE and RMSE. This demonstrated the feasibility of estimating regional patterns of DSL from theoretical temporal stability. Soil texture, OC, FC, MAP and PSD affected the temporal persistence of DSL-SWC and DSLT. This also suggested that soil- and climate-related factors dominated regional temporal persistence of spatial patterns of DSL in the Loess Plateau. Lower soil water holding capacity, fewer precipitation and more concentrated PSD could intensify the formation and/or development of permanent DSL under global climate change.

There was need for future research to further verify the feasibility of estimating long-term regional mean DSL. There is also need to assess temporal persistence of DSL under different land use conditions and climatic zones. Results of such studies could be used to

optimize land use management and mitigate the formation and development of DSL in the Loess Plateau and other regions.

Acknowledgements

This study was financially supported by the National Natural Science Foundation of China (Nos. 41390461 and 51179180). The authors are indebted to the editors and reviewers for their constructive comments and suggestions during the review process of this manuscript. We acknowledge the help of Dr. Liu ZP, Dr. Wang YQ and Ms. Zhu S in designing the experiment, collecting field data and correcting the language.

References

Biswas, A., Si, B.C., 2011. Identifying scale specific controls of soil water storage in a hummocky landscape using wavelet coherency. Geoderma 165, 50–59.
Bosch, D.D., Lakshmi, V., Jackson, T.J., Choi, M., Jacobs, J.M., 2006. Large scale measurements of soil moisture for validation of remotely sensed data: Georgia soil moisture experiment of 2003. J. Hydrol. 323 (1–4), 120–137.
Breshears, D.D., Cobb, N.S., Rich, P.M., Price, K.P., Allen, C.D., Balice, R.G., Romme, W.H., Kastens, J.H., Floyd, M.I., Belnap, J., Anderson, J.J., Myers, O.B., Meyer, C.W., 2005. Regional vegetation die-off in response to global-change-type drought. Proc. Natl. Acad. Sci. USA 102 (42), 15144–15148.
Brocca, L., Melone, F., Moramarco, T., Morbidelli, R., 2009. Soil moisture temporal stability over experimental areas in Central Italy. Geoderma 148, 364–374.
Brocca, L., Tullo, T., Melone, F., Moramarco, T., Morbidelli, R., 2012. Catchment scale soil moisture spatial-temporal variability. J. Hydrol. 422–423, 63–75.
Chen, H.S., Shao, M.A., Li, Y.Y., 2008a. Soil desiccation in the Loess Plateau of China. Geoderma 143, 91–100.
Chen, H.S., Shao, M.A., Li, Y.Y., 2008b. The characteristics of soil water cycle and water balance on steep grassland under natural and simulated rainfall conditions in the Loess Plateau of China. J. Hydrol. 360 (1–4), 242–251.
Fan, J., Shao, M.A., Hao, M.D., Wang, Q.J., 2004. Desiccation and nitrate accumulation of apple orchard soil on the Weibei dryland. J. Appl. Ecol. 15, 1213–1216 (in Chinese with English abstract).
Gao, L., Shao, M.A., 2012. Temporal stability of soil water storage in diverse soil layers. Catena 95, 24–32.
García, I., Mendoza, R., Pomar, M., 2008. Deficit and excess of soil water impact on plant growth of Lotus tenuis by affecting nutrient uptake and arbuscularmycorrhizal symbiosis. Plant Soil 304 (1), 117–131.
Guo, Q., Hu, Z.M., Li, S.G., Li, X.R., Sun, X.M., Yu, G.R., 2012. Spatial variations in aboveground net primary productivity along a climate gradient in Eurasian temperate grassland: effects of mean annual precipitation and its seasonal distribution. Global Change Biol. 18, 3624–3631.
Hu, W., Shao, M.A., Han, F.P., Reichardt, K., Tan, J., 2010a. Watershed scale temporal stability of soil water content. Geoderma 162, 260–272.
Hu, W., Shao, M.A., Reichardt, K., 2010b. Using a new criterion to identify sites for mean soil water storage evaluation. Soil Sci. Soc. Am. J. 74, 762–773.
Hu, W., Tallon, L.K., Si, B.C., 2012. Evaluation of time stability indices for soil water storage upscaling. J. Hydrol. 475, 229–241.
Hupet, F., Vanclooster, M., 2002. Intraseasonal dynamics of soil moisture variability within a small agricultural maize cropped field. J. Hydrol. 261, 86–101.
Jacobs, J.M., Mohanty, B.P., Hsu, E.C., Miller, D., 2004. SME02: field scale variability, time stability and similarity of soil moisture. Remote Sens. Environ. 92, 436–446.
Jia, X.X., Wei, X.R., Shao, M.A., Li, X.Z., 2012. Distribution of soil carbon and nitrogen along a revegetational succession on the Loess Plateau of China. Catena 95, 160–168.
Jia, X.X., Shao, M.A., Wei, X.R., Wang, Y.Q., 2013a. Hillslope scale temporal stability of soil water storage in diverse soil layers. J. Hydrol. 498, 254–264.
Jia, Y.H., Shao, M.A., Jia, X.X., 2013b. Spatial pattern of soil moisture and its temporal stability within profiles on a loessial slope in northwestern China. J. Hydrol. 495, 150–161.
Jin, T.T., Fu, B.J., Liu, G.H., Wang, Z., 2011. Hydrologic feasibility of artificial forestation in the semi-arid Loess Plateau of China. Hydrol. Earth Syst. Sci. 15, 2519–2530.
Jipp, P.H., Nepstad, D.C., Cassel, D.K., Carvalho, C., 1998. Deep soil moisture storage and transpiration in forests and pastures of seasonally-dry Amazonia. Clim. Change 39, 395–412.
Kachanoski, R.G., de Jong, E., 1988. Scale dependence and the temporal stability of spatial patterns of soil water storage. Water Resour. Res. 24, 85–91.
Klute, A., Dirksen, C., 1986. Hydraulic conductivity of saturated soils. In: Klute, A. (Ed.), Methods of Soil Analysis. ASA and SSSA, Madison, Wisconsin, USA, pp. 694–700.
Li, Y.S., 1983. The properties of water cycle in soil and their effect on water cycle for land in the Loess Plateau. Acta Ecol. Sin. 3 (2), 91–101 (in Chinese with English abstract).
Liu, B.X., Shao, M.A., 2014. Estimation of soil water storage using temporal stability in four land uses over 10 years on the Loess Plateau, China. J. Hydrol. 517, 974–984.
Martínez-Fernández, J., Ceballos, A., 2003. Temporal stability of soil moisture in a large-field experiment in Spain. Soil Sci. Soc. Am. J. 67, 1647–1656.
Nelson, D.W., Sommers, L.E. (Eds.), 1982. Total carbon, organic carbon and organic matter. In: Page, A.L., Miller, R.H., Keeney, D.R. (Eds.), Methods of Soil Analysis. Part 2. Agronomy Monograph, second ed. ASA and SSSA, Madison, WI. pp. 534–580.
Pollen, N., 2007. Temporal and spatial variability in root reinforcement of stream banks: accounting for soil shear strength and moisture. Catena 69 (3), 197–205.
Ratliff, L.F., Ritchie, J.T., Cassel, D.K., 1983. Field-measured limits of soil water availability as related to laboratory-measured properties. Soil Sci. Soc. Am. J. 47, 770–775.
Robinson, N., Harper, R., Smettem, K., 2006. Soil water depletion by Eucalyptus spp. integrated into dryland agricultural systems. Plant Soil 286 (1), 141–151.
Schneider, K., Huisman, J.A., Breuer, L., Zhao, Y., Frede, H.G., 2008. Temporal stability of soil moisture in various semi-arid steppe ecosystems and its application in remote sensing. J. Hydrol. 359, 16–29.
Shi, H., Shao, M.A., 2000. Soil and water loss from the Loess Plateau in China. J. Arid Environ. 45, 9–20.
Starks, P.J., Heathman, G.C., Jackson, T.J., Cosh, M.H., 2006. Temporal stability of soil moisture profile. J. Hydrol. 324, 400–411.
Tsunekawa, A., Liu, G.B., Yamanaka, N., Du, S., 2014. Restoration and Development of the Degraded Loess Plateau. Springer, China.
Vachaud, G., Passerat de Silans, A., Balabanis, P., Vauclin, M., 1985. Temporalstability of spatially measured soil water probability density function. Soil Sci. Soc. Am. J. 49, 822–828.
Vanderlinden, K., Vereecken, H., Hardelauf, H., Herbst, M., Martínez, G., Cosh, M.H., Pachepsky, Y.A., 2011. Temporal stability of soil water contents: a review of data and analyses. Vadose Zone J. http://dx.doi.org/10.2136/vzj2011.0178.
Wang, Z.Q., Liu, B.Y., Liu, G., Zhang, R.X., 2009. Soil water depletion depth by planted vegetation on the Loess Plateau. Sci. China Earth Sci. 52, 835–842.
Wang, Y.Q., Shao, M.A., Liu, Z.P., 2010a. Large-scale spatial variability of dried soil layers and related factors across the entire Loess Plateau of China. Geoderma 159, 99–108.
Wang, Y.Q., Shao, M.A., Shao, H.B., 2010b. A preliminary investigation of the dynamic characteristics of dried soil layers on the Loess Plateau of China. J. Hydrol. 381, 9–17.
Wang, Y.Q., Shao, M.A., Zhu, Y.J., Liu, Z.P., 2011a. Impacts of land use and plant characteristics on dried soil layers in different climatic regions on the Loess Plateau of China. Agr. Forest Meteorol. 151, 437–448.
Wang, X.C., Muhammad, T.N., Hao, M.D., Li, J., 2011b. Sustainable recovery of soil desiccation in semi-humid region on the Loess Plateau. Agr. Water Manage. 98, 1262–1270.
Wang, Y.Q., Shao, M.A., Liu, Z.P., Warrington, D.N., 2012a. Investigation of factors controlling the regional-scale distribution of dried soil layers under forestland on the Loess Plateau, China. Surv. Geophys. 33, 311–330.
Wang, X.C., Li, J., Muhammad, T.N., Fang, X.Y., 2012b. Validation of the EPIC model and its utilization to research the sustainable recovery of soil desiccation after alfalfa (*Medicago sativa L.*) by grain crop rotation system in the semi-humid region of the Loess Plateau. Agr. Ecosyst. Environ. 161, 152–160.
Wang, Q.X., Fan, X.H., Qin, Z.D., Wang, M.B., 2012c. Changes trends of temperature and precipitation in the Loess Plateau Region of China, 1961–2010. Global Planet Change 92–93, 138–147.
Yang, W.Z., 2001. Soil water resources and afforestation in Loess Plateau. J. Nat. Resour. 16 (5), 433–438 (in Chinese with English abstract).
Yang, W.Z., Han, S.F., 1985. Soil water ecological environment on the artificial woodland and grassland in Loess hilly region. Memoir NISWC, Acad. Sin. Ministry Water Conserv. 2, 18–28 (in Chinese with English abstract).
Yang, Q.Y., Zhang, B.P., Zheng, D., 1988. On the boundary of the Loess Plateau. J. Nat. Resour. 3, 9–15 (in Chinese with English abstract).
Yu, H., 1992. Characteristics of water resource in the Loess Plateau and their countermeasures for utilization. Arid Land Geogr. 15 (3), 59–64 (in Chinese with English abstract).
Zhao, Y., Peth, S., Wang, X.Y., Lin, H., Horn, R., 2010. Controls of surface soil moisture spatial patterns and their temporal stability in a semi-arid steppe. Hydrol. Process. 24, 2507–2519.